

Precise Measurements of the Proton and Deuteron
Structure Functions from a Global Analysis of the SLAC
Deep Inelastic Electron Scattering Cross Sections*

L. W. Whitlow, E. M. Riordan,[◇] S. Dasu
*Stanford Linear Accelerator Center,
Stanford University, Stanford, California 94309*

S. Rock
The American University, Washington, DC 20016

A. Bodek
University of Rochester, Rochester, New York 14627

Abstract

We report new values of the proton and deuteron structure functions $F_2(x, Q^2)$ based on a global analysis of eight SLAC experiments on deep inelastic $e-p$ and $e-d$ scattering. These functions were determined over the entire SLAC kinematic range: $0.06 \leq x \leq 0.9$ and $0.6 \leq Q^2 \leq 30.0$ (GeV/c)². The data are compared with high- Q^2 measurements of $F_2(x, Q^2)$ made in deep inelastic $\mu-p$ and $\mu-d$ scattering experiments at CERN. New results for the ratio F_2^n/F_2^p are also reported.

Submitted to Physics Letters B

* This research was supported in part by Department of Energy contracts DE-AC03-76SF00515 and DE-AC02-7-6ER13065, by National Science Foundation Grant PHY85-10549, and by Lawrence Livermore National Laboratories-Stanford University Research Participation Agreement No. 6936905.

◇ Current address: Universities Research Association, Washington, DC 20036.

I. Introduction

Between 1970 and 1985 a series of eight experiments [1-8] at SLAC provided detailed knowledge of the deep inelastic $e-p$, $e-d$ and $e-n$ scattering cross sections. The extraction of the structure function F_2 from these cross sections is, however, sensitive to the radiative corrections and to the value of $R = \sigma_L/\sigma_T$, especially in the SLAC kinematic range, where R is known [4,6] to be substantial. New precise measurements [9,10] of $R(x, Q^2)$ and improved radiative correction procedures [10-12] now permit the extraction of $F_2(x, Q^2)$ from the early SLAC experiments with significantly improved accuracy. In addition, the relative normalization of all these SLAC experiments has been determined, reducing the corresponding uncertainty in F_2 .

Recent high- Q^2 measurements of $F_2(x, Q^2)$ in deep inelastic $\mu-p$ and $\mu-d$ scattering by the BCDMS collaboration [13] at CERN are inconsistent with earlier measurements made by the EMC collaboration [14]. This disparity could not be resolved by comparisons with a subset of the old SLAC F_2 measurements [4] because the CERN and that SLAC data span essentially disjoint ranges of Q^2 . Accurate knowledge of the nucleon structure functions is required to determine the momentum distributions of quarks within the proton and neutron. In Perturbative QCD (PQCD) calculations of hadron-hadron interactions the square of the quark distribution is convoluted with the quark-quark scattering cross section. The two inconsistent CERN measurements [13,14] of F_2 have led to quark distributions [15,16] that differ by up to 10%. The current analysis resolves this discrepancy.

Comparisons of the ratio F_2^n/F_2^p between the BCDMS [17] and EMC results [18] also show substantial differences (although consistent within systematic errors). This disparity leads to large uncertainties in PQCD calculations that are sensitive to the ratio of up to down quark distributions. Ratios of F_2^n/F_2^p from a previous SLAC study [4]

appear to be uniformly larger than both the EMC and BCDMS results, but the SLAC data occur at lower Q^2 , suggesting the possibility of a significant Q^2 -dependence in the ratio.

We report here new determinations of F_2 from a combined reanalysis of 3020 $e-p$ and 2815 $e-d$ cross section measurements, each of typically $\pm 3\%$ statistical accuracy, from eight experiments [1-8] using the 1.6 GeV, 8 GeV, and 20 GeV spectrometers at the SLAC End Station A facility [19]. Ratios of F_2^n/F_2^p are derived from a reanalysis of 2744 deuteron/proton cross section ratios measured at identical kinematics in six of these experiments, using the same apparatus for both measurements. The present analysis benefits from a much improved radiative corrections procedure and a precise method of normalizing the experimental data sets to one another. The extracted values of F_2 and F_2^n/F_2^p span the entire SLAC kinematic range, $0.06 \leq x \leq 0.90$ and $0.6 \leq Q^2 \leq 30.0$ (GeV/c)², and overlap with the EMC and BCDMS datasets for $x \geq 0.25$, permitting a direct comparison of SLAC and CERN measurements.

In the first Born approximation, the deep inelastic scattering cross section can be written in terms of the structure functions F_2 and R as

$$\frac{d^2\sigma}{d\Omega dE'} = \frac{4\alpha^2 E'^2 \cos^2(\theta/2)}{Q^4} \frac{1}{\nu} F_2(x, Q^2) \left[1 + \frac{1-\epsilon}{\epsilon} \frac{1}{1+R(x, Q^2)} \right], \quad (1)$$

where E is the energy of the incident electron, θ the scattering angle, E' the final electron energy in the lab frame; $\nu = E - E'$ is the energy transfer; $Q^2 = 4EE' \sin^2(\theta/2)$ is the invariant four-momentum transfer squared; $x = Q^2/2M\nu$ is the Bjorken scaling variable; $\epsilon = [1 + 2(1 + \nu^2/Q^2) \tan^2(\theta/2)]^{-1}$ is the polarization of the exchanged virtual photon; and M is the mass of the proton. By assuming or measuring a functional form for R , one can extract values of F_2 from the measured differential cross sections.

The global analysis procedure is described in detail in refs. [9] and [10]. First we corrected all cross sections for radiative effects according to the Bardin/Tsai prescription [8,10-12]. Then we normalized the individual data sets to one another by separately fitting all proton and all deuteron cross section measurements and all ratios of σ^d/σ^p to smoothly varying functions with variable normalization parameters [9,10]. The best-fit normalization factors with statistical and systematic uncertainties were presented in table 1 of ref. [10]. Then $R(x, Q^2)$ was determined from the corrected cross sections measured at the same (x, Q^2) but for different ϵ . We then used an empirical parameterization of R to extract $F_2(x, Q^2)$ from each measured cross section using eq. (1). In this way we obtained coherent SLAC data sets for F_2^p , F_2^d , and F_2^d/F_2^p .

Throughout these analyses we employed a detailed propagation of all known systematic uncertainties. The principal sources of systematic error in the F_2 data are: the uncertainty in the overall normalization of the combined SLAC data, $\pm 2.1\%$ for the proton and $\pm 1.7\%$ for the deuteron; uncertainties in the relative normalizations of the experiments, typically $\pm 1.1\%$; an ϵ -dependent uncertainty due to the radiative corrections, which is estimated [9] to be everywhere less than $\pm 0.5\%$; the experimental uncertainty in the functional form assumed for R , which contributes between $\pm 0.3\%$ and $\pm 2.0\%$ in F_2 , except at very large scattering angles, where it contributes about as much as the statistical error in the cross section. Consult ref. [9] for a complete discussion of the full nine-component F_2 "error vector" and its propagation through the analysis.

Because $R_d = R_p$, [10] we obtained F_2^d/F_2^p directly from σ^d/σ^p at each kinematic point where both cross sections are available. The principal sources of systematic error in the F_2^d/F_2^p ratios are [20] the overall normalization uncertainty of $\pm 1.0\%$ and the relative normalization uncertainties of the different experiments, typically $\pm 0.6\%$.

The resulting SLAC data sets contain values of F_2 and F_2^d/F_2^p at specific (x, Q^2) points distributed throughout the SLAC kinematic range. To compare them with the

EMC and BCDMS results, we have grouped the SLAC data into appropriate x -bins and applied a bin-centering correction using a best-fit model to our data (see below).

Figures 1 and 2 present the SLAC data for F_2^p in x -bins that match those of EMC and BCDMS respectively; the corresponding data for F_2^d are shown in figs. 3 and 4. These new results are in excellent agreement with the previous SLAC values [4], but they span a substantially greater kinematic range and have much reduced errors. Tables of $F_2(x, Q^2)$ are available in ref. [9].

- We determined the relative normalization of SLAC and EMC F_2 [9] by fitting the combined SLAC and EMC F_2^p and F_2^d data sets to several structure function models each with a variable normalization parameter. The average best-fit normalization factor of SLAC/ EMC = $1.07 \pm 0.01(\text{stat}) \pm 0.02(\text{sys})$. The second error represents the systematic uncertainty due to model choice and kinematic cuts. The χ^2/df for all fits are less than one for both hydrogen and deuterium. Within the errors the relative normalization factors for hydrogen and deuterium are the same. The results of this normalization are shown in figs. 1 and 3. The EMC results [14] for F_2 (assumed $R = 0$) were corrected upward by up to 5% at low x to reflect the new $R(x, Q^2)$ values of ref. [10] and were multiplied by 1.07. With this normalization correction, we observe good agreement between the new SLAC results and those of EMC wherever the two data sets overlap ($0.175 \leq x \leq 0.65$).

In figs. 2 and 4 we compare the SLAC results with those of BCDMS [13] (assumed $R = R_{QCD}$), which were corrected by less than 1% to reflect the new $R(x, Q^2)$ values and normalized by a factor of 1.00. We observe generally good agreement between the SLAC and BCDMS data, with two possible exceptions. First, the lowest- Q^2 data of BCDMS at $x = 0.55$ and $x = 0.65$ are lower than the SLAC data in these regions. This difference could be due to a possible $\approx 1.5\sigma$ correlated systematic shift in the BCDMS data due to beam energy or spectrometer calibration or resolution [21]. Such a shift only effects

the BCDMS high- x low- Q^2 kinematic region. Second, at $x = 0.225$ and $x = 0.275$, while there is no overlap between the experiments, the tendency of the SLAC data appears lower than that of the BCDMS data. We determined the relative normalization of the SLAC and BCDMS experiments by overall fits to both data sets (similar to the fits used for the EMC data). The relative normalization of the two experiments is $1.00 \pm 0.01(\text{stat}) \pm 0.03(\text{sys})$. The χ^2/df is slightly larger than unity due to the discrepancies mentioned above. The systematic error has been enhanced due to the quality of the fit.

The dashed lines in figs. 2 and 4 are the values of F_2^p and F_2^d obtained directly from the Next to Leading Order (B1-DIS-scheme fit) quark distributions of Morfin and Tung [15] which were extracted from the BCDMS F_2 and other data (not including EMC). The solid line includes the target mass effects [22]. As expected the curves match the BCDMS data very well, especially in the region of the fit [above $Q^2 = 10 \text{ (GeV/c)}^2$]. Unfortunately the curves follow the systematic offsets of the BCDMS data at high x . At low x the curves are higher than the low Q^2 data while at high x the curves are significantly lower than the SLAC data. At low Q^2 , the calculated F_2^p shows large target mass effects that lessen the disagreements with SLAC data. The difference between the PQCD + target mass solid curve and the data may be due to dynamic higher twist effects. These trends are consistent with the observations of BCDMS [21] from their combined NLO PQCD fit to both the SLAC and their own data.

The SLAC $F_2^p(x, Q^2)$ and $F_2^d(x, Q^2)$ can be parameterized by:

$$F_2^{fit}(x, Q^2) = \beta F_2^{thr}(x) \left\{ 1 + \lambda_1(x) \log \left[\frac{Q^2}{A(x)} \right] + \lambda_2(x) \log^2 \left[\frac{Q^2}{A(x)} \right] \right\}, \quad (2)$$

where

$$F_2^{thr}(x) = \sum_{i=1}^5 C_i (1-x)^{i+2},$$

$$\lambda_1(x) = \sum_{i=0}^3 C_{i+9} x^i,$$

$$\lambda_2(x) = \begin{cases} C_6 + C_7 x + C_8 x^2, & \text{if } Q^2 \leq A(x), \\ 0, & \text{otherwise,} \end{cases}$$

$$A(x) = 1.22 e^{3.2x},$$

$$\beta = \begin{cases} [1 - \exp(-\min\{20, 7.7[1/x + M_p^2/Q^2 - 1]\})]^{-1}, & \text{deuterium,} \\ 1, & \text{hydrogen.} \end{cases}$$

This parameterization is valid in the kinematic region bounded by $x \geq 0.062$, $Q^2 \geq 0.6 \text{ (GeV/c)}^2$, $\nu \leq 19 \text{ GeV}$ and $W^2 \geq 3 \text{ GeV}^2$, where $W^2 = M^2 + Q^2 \cdot (1/x - 1)$ is the mass of the hadronic final state. The cut at $W^2 = 3 \text{ GeV}^2$ assures that eq. 2 is sufficient to fit the data without additional nucleon resonance parameters.

To determine the parameters C_i the unbinned structure function data were condensed by combining different measurements (from the same experiment) at nearly the same kinematics. This procedure improves the propagation of most systematic errors through the fitting procedure while reducing the data to 661 F_2^p and 691 F_2^d measurements. Best fit coefficients for F_2^{fit} are given in table 1. The observed χ^2 per degree-of-freedom, based on the quadrature sum of statistical and systematic errors, is 506/652 for the proton and 438/682 for the deuteron data.

The ratio of neutron to proton structure functions can be obtained from F_2^d and F_2^p by properly correcting for the effects of the deuteron wave function and possible EMC effects. We have followed the standard procedure of Frankfurt and Strikman [23] and

used the Paris [24] wave function for the deuteron. The measured F_2^p was smeared and then subtracted from the measured F_2^d to yield a smeared neutron structure function, F_{2s}^n . An iteration procedure was used to determine the neutron smearing correction $S_n = F_{2s}^n/F_2^n$. Values of S_n and S_p , the corresponding smearing correction for the proton, are within 0.5% of unity for $x \leq 0.45$. At $x = 0.85$, S_n and S_p decrease with Q^2 and are 0.67 and 0.78 respectively at $Q^2 = 20$ (GeV/c)². The values of F_2^n/F_2^p are independent (within 1%) of the assumed deuteron wave function for $x \leq 0.65$. However, at larger values of x there is significant model dependence. The values of F_2^n/F_2^p at $x = 0.85$ are $\sim 20\%$ higher using the Bonn [25] wave function and $\sim 15\%$ lower using the Reid Soft Core [26] wave function compared to the Paris wave function. At $x = 0.75$ the variation due to choice of wave function is $\sim \pm 4\%$.

An alternate approach to extracting the neutron structure function based on the EMC effect has been given more recently by Frankfurt and Strikman [27] They estimate that $F_2^d/(F_2^p + F_2^n) - 1$, the EMC effect in the deuteron, is approximately 25% of the EMC effect in iron [7]. Present limits on the EMC effect in the deuteron, extracted from a comparison of electron scattering data on deuterium to neutrino and anti-neutrino data on hydrogen [28] are not stringent enough to differentiate between the two smearing options. Table 2 gives F_2^n/F_2^p for both methods at a few kinematic values. Because the results from the alternate method are completely different at high x from those obtained using the standard method and since the standard unfolding procedure has been used by previous experimental groups, we will ignore the alternate approach in the rest of this paper. However, this is a warning that at high x more theoretical analysis is necessary to understand the deuteron.

The ratio F_2^n/F_2^p extracted using the Paris wave function is plotted in fig. 5 as a function of x for two ranges of Q^2 . The outer error bars include the substantial uncertainty due to the choice of wave function. F_2^n/F_2^p approaches unity at low x and falls very close to the limiting value of 0.25 at the highest x . In the mid- x region,

where there data from both ranges of Q^2 is shown, there is a visible Q^2 dependence to F_2^n/F_2^p . To determine this Q^2 dependence we calculated $d[F_2^n/F_2^p]/d[\ln Q^2]$ from a fit of the form $F_2^n/F_2^p = a + b \cdot \ln Q^2$ to the SLAC data with $W^2 \geq 3.5 \text{ GeV}^2$. As shown in fig. 6, this logarithmic derivative is less than zero for $x \leq 0.6$. We also show here the results of a combined fit to SLAC and BCDMS [17] F_2^n/F_2^p . Both fits have χ^2/df close to one and both agree in sign and magnitude. Thus the apparent discrepancy in F_2^n/F_2^p between high energy CERN data and the lower energy SLAC data must be the result of a significant Q^2 dependence. This is not included in the quark distributions of Morfin and Tung. The Stockholm diquark model [29] is consistent with the observed Q^2 dependence.

In conclusion, these new SLAC values of $F_2(x, Q^2)$ from deep inelastic electron scattering are $\approx 7\%$ higher than the muon scattering results of EMC and are in good agreement with the results of BCDMS (when corrected for a systematic shift in their magnetic field). A re-analysis of the EMC data [30] gives results that are several percent higher than the old analysis and thus in better agreement with both the SLAC and BCDMS data. The combined SLAC/BCDMS results now provide a consistent data set from the low Q^2 edge of the deep inelastic scattering regime to the high Q^2 regime.

Acknowledgement

We would like to thank the members of Group A and the Spectrometer Facilities Group at SLAC for their assistance and for their excellent archival efforts.

References

- [1] J.S. Poucher et al., Phys. Rev. Lett. 32 (1974) 118; J.S. Poucher, Ph.D. thesis, Massachusetts Institute of Technology, MIT-LNS (1971); see also ref. [4].
- [2] A. Bodek et al., Phys. Rev. Lett. 30 (1973) 1084; E.M. Riordan et al., Phys. Rev. Lett. 33 (1974) 561; E.M. Riordan, Ph.D. thesis, Massachusetts Institute of Technology, MIT-LNS Report COO-3069-176 (1973); A. Bodek, Ph.D. thesis, Massachusetts Institute of Technology, MIT-LNS Report COO-3069-116 (1972); see also ref. [4].
- [3] S. Stein et al., Phys. Rev. D11 (1975) 1884.
- [4] A. Bodek et al., Phys. Rev. D21 (1979) 1471.
- [5] W.B. Atwood et al., Phys. Lett. B64 (1976) 479; W.B. Atwood, Ph.D. thesis, Stanford University, SLAC-Report-185 (1975).
- [6] M.D. Mestayer et al., Phys. Rev. D27 (1983) 285; M.D. Mestayer Ph.D. thesis, Stanford University, SLAC-Report-214 (1978).
- [7] R.G. Arnold et al., Phys. Rev. Lett. 52 (1984) 727; J.G. Gomez, Ph.D. thesis, The American University (1987).
- [8] S. Dasu et al., Phys. Rev. Lett. 61 (1988) 1061; S.R. Dasu, Ph.D. thesis, University of Rochester Report UR-1059 (1988). See also ref. [9], which gives improved results.
- [9] L.W. Whitlow, Ph.D. thesis, Stanford University, SLAC-Report-35 (1990); for full data tables request Appendix E, available on 5 1/2-inch IBM PC/AT, 3 1/2-inch IBM PS/2, and 3 1/2-inch Apple Macintosh diskettes.
- [10] L.W. Whitlow et al., Phys. Lett. B250 (1990) 193; for details see ref. [9].

- [11] Y.S. Tsai, Rev. Mod. Phys. 46 (1974) 815; SLAC-PUB-848 (1971); and Phys. Rev. 122 (1961) 1898; L.W. Mo and Y.S. Tsai, Rev. Mod. Phys. 41 (1969) 295.
- [12] A.A. Akhundov, D. Yu. Bardin, and W. Lohman, JINR E2-86-204 (1986); A.A. Akhundov, D. Yu Bardin, and N.M. Shumeiko, Sov. J. Nucl. Phys. 44 (1986) 1212 and 26 (1977) 660; D. Yu Bardin and N.M. Shumeiko, Sov. J. Nucl. Phys. 29 (1979) 499.
- [13] A.C. Benvenuti et al., Phys. Lett. B223 (1989) 485; Phys. Lett. B237 (1990) 592.
- [14] J.J. Aubert et al., Nucl. Phys. B259 (1985) 189.
- [15] J.G. Morfin and Wu-ki Tung, Fermilab-Pub-90/74, Submitted to Z. Phys. C.
- [16] P.N. Harriman, A.D. Martin, W.J. Stirling and R.G. Roberts, Phys. Rev. D42 (1990) 798.
- [17] A.C. Benvenuti et al., Phys. Lett. B237 (1990) 599; and private communication, M. Virchaux.
- [18] J.J. Aubert et al., Nucl. Phys. B293 (1987) 740.
- [19] NPAS Users Guide, SLAC-Report-269 (1984); see also ref. [4].
- [20] A separate study of the relative normalizations of the six experimental data sets of F_2^d/F_2^p ratios is in good agreement with the results of ref. [9], but yields smaller uncertainties due to the cancellation of most systematic errors.
- [21] A. Milsztajn et al., Z. Phys. C49 (1991) 527.
- [22] H. Georgi and H.D. Politzer, Phys. Rev. D14 (1976) 1829.
- [23] L.L. Frankfurt and M.I. Strikman, Phys. Rep. 76 (1981) 215; see eqs. (3.10) and (3.11).
- [24] M. Lacombe et al., Phys. Lett. 101B (1981) 139.

- [25] R. Machleidt, K. Holinde and C. Elster, Phys. Rep. 149 (1987) 1.
- [26] R.V. Reid, Ann. Phys. (NY) 50 (1968) 411.
- [27] L.L. Frankfurt and M.I. Strikman, Phys. Rep. 160 (1988) 235. See eq. (3.25).
- [28] A. Bodek and A. Simon, Z. Phys. C29 (1985) 231.
- [29] S. Ekelin and S. Fredriksson, Phys. Lett. 162B (1985) 373.
- [30] Private communication, J. Wimpenny.

Table I. Best fit coefficients for $F_2^{fit}(x, Q^2)$. The total observed χ^2 is 506 based on 652 degrees of freedom.

Coefficient	Hydrogen	Deuterium
C_1	1.417 ± 0.039	0.948 ± 0.027
C_2	-0.108 ± 0.311	-0.115 ± 0.215
C_3	1.486 ± 0.903	1.861 ± 0.624
C_4	-5.979 ± 1.106	-4.733 ± 0.762
C_5	3.524 ± 0.482	2.348 ± 0.333
C_6	-0.011 ± 0.025	-0.065 ± 0.024
C_7	-0.619 ± 0.153	-0.224 ± 0.144
C_8	1.385 ± 0.213	1.085 ± 0.193
C_9	0.270 ± 0.028	0.213 ± 0.024
C_{10}	-2.179 ± 0.221	-1.687 ± 0.183
C_{11}	4.722 ± 0.537	3.409 ± 0.439
C_{12}	-4.363 ± 0.405	-3.255 ± 0.333

Table II. Smearing corrections to F_2^d/F_2^p to obtain F_2^n/F_2^p . Column 4 gives the results by the standard method using the Paris Potential. Column 5 shows the ratio of F_2^n/F_2^p extracted using the Reid or Bonn Potentials to using the Paris Potential. Column 7 is F_2^n/F_2^p obtained using the alternate method based on the EMC effect. The errors in n/p are ± 0.01 for $x \leq 0.75$ and ± 0.03 for $x = 0.85$.

x	$\langle Q^2 \rangle$	F_2^d/F_2^p No Smearing Correction	F_2^n/F_2^p			
			Standard Method [22]			Alternate Method [26]
			Paris	Reid/Paris	Bonn/Paris	
0.275	4.7	1.69	0.70	1.000	0.997	0.69
0.35	6.3	1.61	0.62	0.999	0.997	0.61
0.45	9.3	1.54	0.55	0.997	0.997	0.56
0.55	11.5	1.48	0.48	0.995	0.998	0.52
0.65	13.6	1.44	0.42	0.990	1.014	0.49
0.75	17.9	1.47	0.35	0.966	1.049	0.50
0.85	23.6	1.74	0.28	0.886	1.250	0.69

Figure Captions

- Figure 1. SLAC values of F_2^p binned according to the x -bins of EMC. The EMC data [12] plotted here were multiplied by the normalization factor 1.07. There are no EMC data at $x = 0.85$.
- Figure 2. SLAC values of F_2^p binned according to the x -bins of BCDMS. The BCDMS data [11] plotted here were multiplied by the normalization factor 1.00. There are no BCDMS data at $x = 0.85$.
- Figure 3. SLAC values of F_2^d binned according to the x -bins of EMC. The EMC data [12] plotted here were multiplied by the normalization factor 1.07. There are no EMC data at $x = 0.85$.
- Figure 4. SLAC values of F_2^d binned according to the x -bins of BCDMS. The BCDMS data [11] plotted here were multiplied by the normalization factor 1.00. There are no BCDMS data at $x = 0.85$.
- Figure 5. F_2^n/F_2^p as a function of x for average values of Q^2 of 3 (GeV/c)² (dash) and 12 (GeV/c)² (solid). The Paris wave function was used to unsmear the deuteron.
- Figure 6. $d[F_2^n/F_2^p]/d[\ln Q^2]$ as a function of x , as extracted from fits to the SLAC data and the combined SLAC BCDMS data.

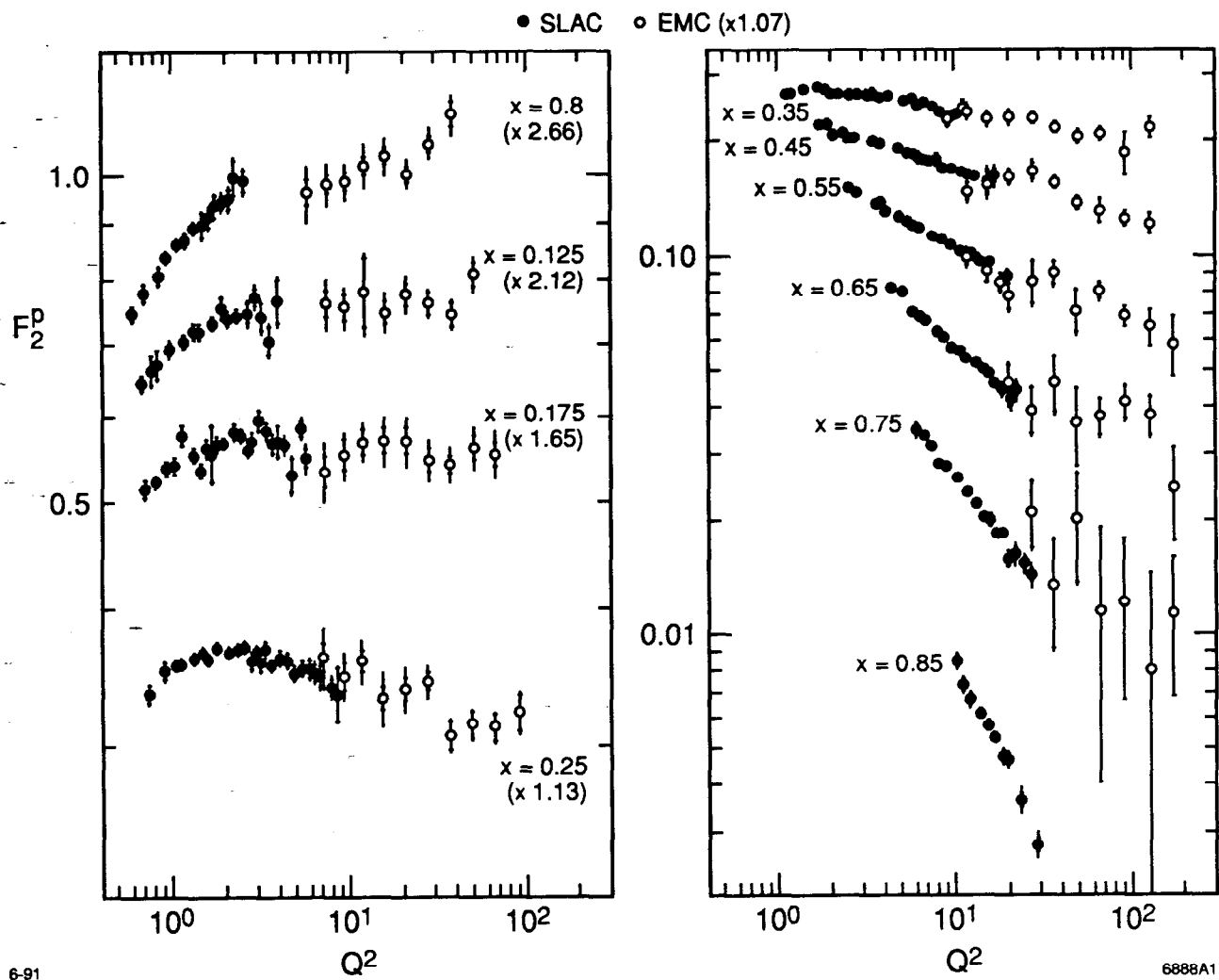


Fig. 1

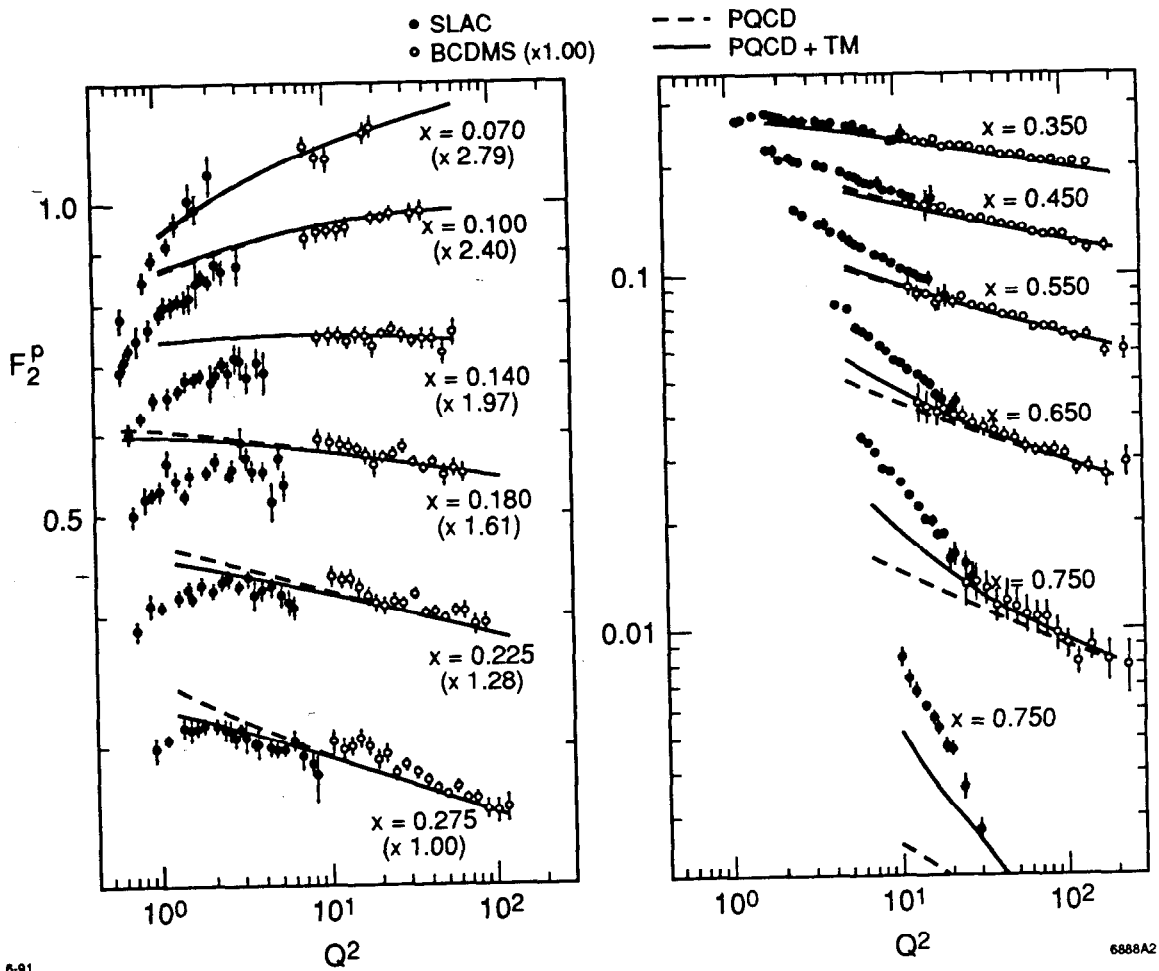


Fig. 2

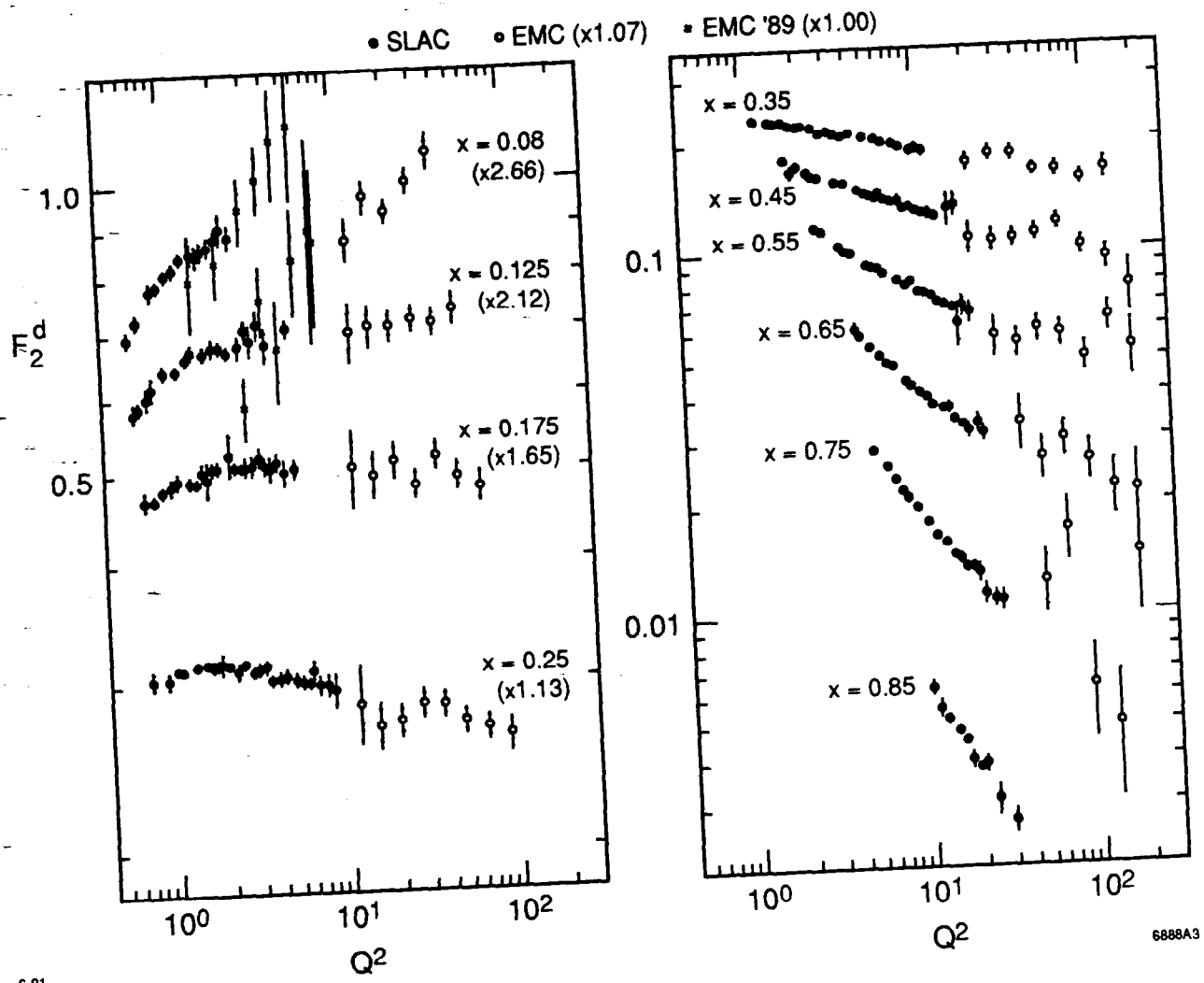


Fig. 3

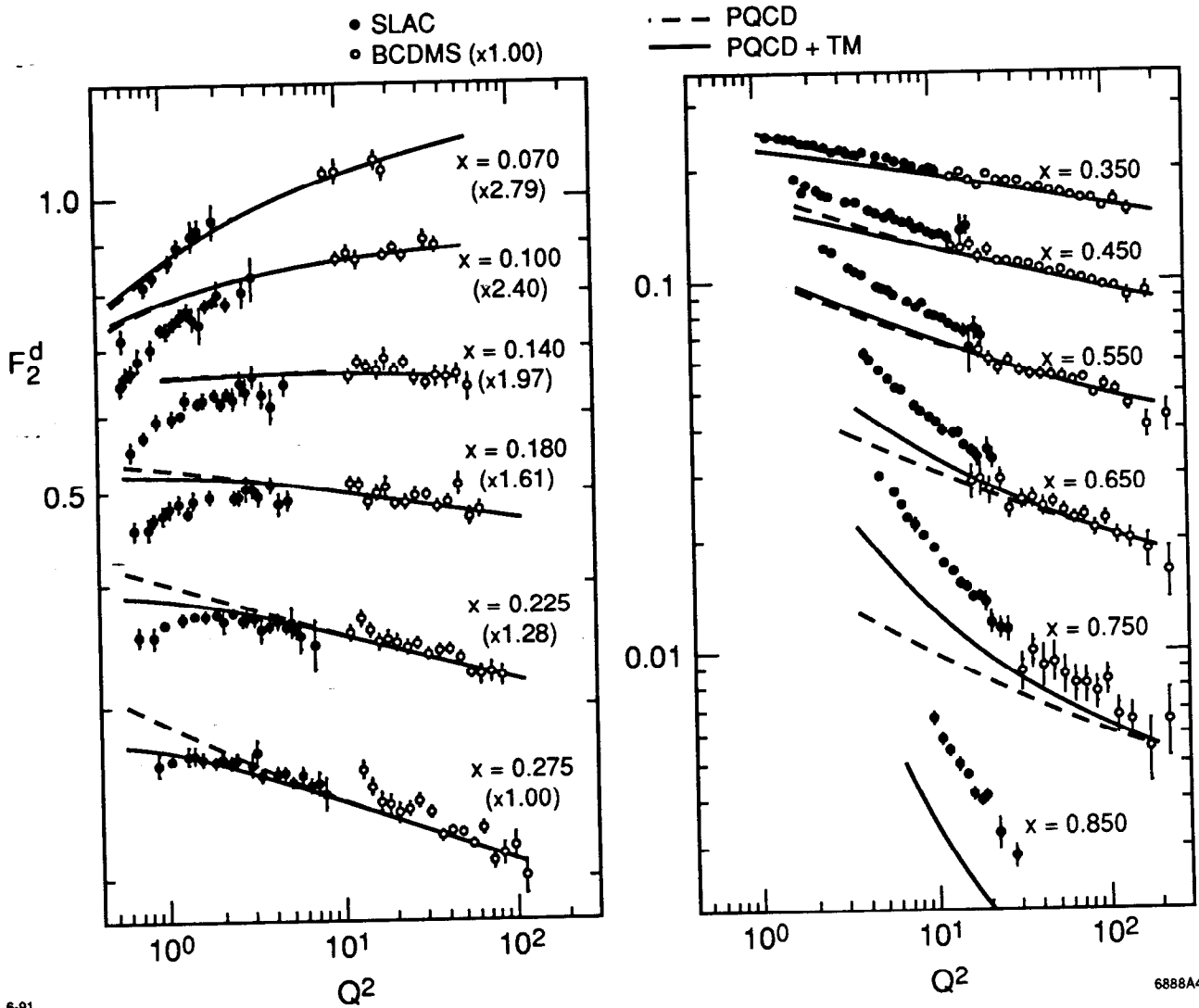


Fig. 4

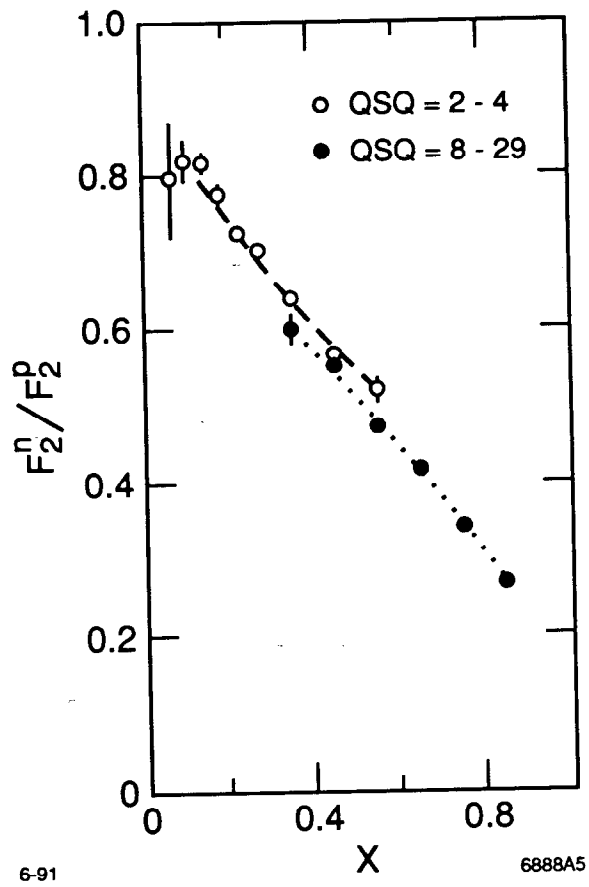
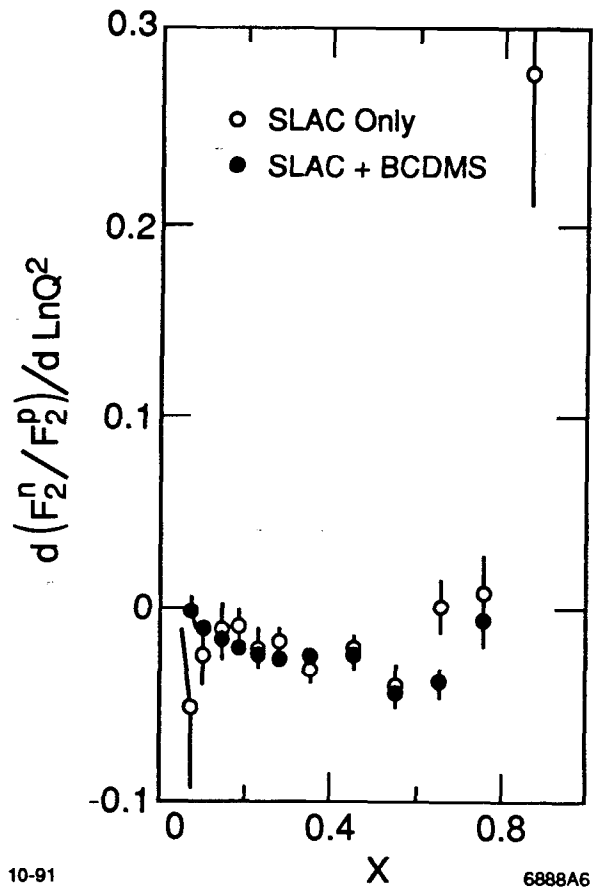


Fig. 5



10-91

6888A6

Fig. 6